

Unveiling Downstream Performance Scaling of LLMs: A Clustering-Based Perspective

Chengyin Xu^{*,†}, Kaiyuan Chen^{*}, Xiao Li, Ke Shen[†], Chenggang Li

ByteDance Seed

^{*}Equal Contribution, [†]Corresponding authors

Abstract

The escalating scale and cost of Large Language Models (LLMs) training necessitate accurate pre-training prediction of downstream task performance for efficient resource allocation. This is challenged by: 1) the emergence phenomenon, where metrics become meaningful only after extensive training, hindering prediction by smaller models; and 2) uneven task difficulty and inconsistent performance scaling patterns, leading to high metric variability. Current prediction methods lack accuracy and reliability. We propose a Clustering-On-Difficulty (COD) framework for downstream performance prediction. The COD framework clusters tasks by their difficulty scaling features, thereby establishing a more stable and predictable support subset through the exclusion of tasks exhibiting non-emergent behavior or irregular scaling. We adopt a performance scaling law to predict cluster-wise performance with theoretical support. Predictable subset performance acts as an intermediate predictor for the full evaluation set. We further derive a mapping function to accurately extrapolate the performance of the subset to the full set. Applied to an LLM with 70B parameters, COD achieved a 1.36% average prediction error across eight key LLM benchmarks, offering actionable insights for resource allocation and training monitoring of LLMs pretraining.

Date: October 14, 2025

Correspondence: Chengyin Xu at xuchengyin.98@bytedance.com, Ke Shen at shenke@bytedance.com

1 Introduction

Large Language Models (LLMs) have emerged as transformative technologies in natural language understanding, generation, and reasoning [1, 6, 18]. Their impressive success heavily relies on scaling model parameters and pre-training data, with training loss empirically following a power-law relationship with compute [22, 25]. However, this reduction in training loss primarily reflects an in-domain compression effect and does not necessarily indicate improved out-of-domain generalization or downstream performance—the factor of primary concern in practice. Specifically, performance scaling of downstream tasks aims to predict the accuracy of the target LLM on downstream tasks using metrics from smaller models. Our objective is to develop a prediction method that works reliably on a diverse range of downstream tasks, optimizing the worst-case prediction error.

Despite extensive efforts, a reliable *scaling law for downstream tasks* remains elusive. One line of work attempts to extrapolate the performance of a large model by modeling the performance-loss relationship [8, 11, 16, 31, 43], but this often fails to capture the emergent behaviors of LLMs and the mismatch between the in-domain loss and downstream metrics [49]. Another line of research focuses on direct extrapolation of the performance-

compute relationship [1, 23], yet a single family of curves usually fails to capture the performance on evaluation benchmarks with complex difficulty distributions across samples.

A critical oversight in current approaches is the assumption of uniform scaling behavior across diverse evaluation samples. We observe that different evaluation samples actually follow distinct performance scaling patterns, and thus applying a single extrapolation formula to the entire evaluation set is suboptimal. We give a detailed analysis in Sec. 3.

To address these challenges, we propose a new performance scaling law, derived from the existing loss scaling law [25], specifically applicable to evaluation subsets that exhibit consistent performance scaling patterns. Building on the performance scaling law, we develop a *Clustering-On-Difficulty* (COD) multi-stage framework for predicting downstream performance. Specifically, we first filter out clusters that lack scaling properties using an improved MeanShift clustering algorithm. Next, we fit the performance-compute relationships in the remaining clusters under our performance scaling law, extrapolate the performance of large models within these clusters, and finally map the aggregated predictions to the complete task set.

We validate our COD approach on eight popular evaluation sets, including MATH [19], BBH [38], and MMLU pro [41] datasets. COD achieves an average prediction error of 1.36%ha on an LLM with 70B parameters. Our results demonstrate that this difficulty-aware framework substantially outperforms existing methods, establishing a promising paradigm for accurate downstream performance scaling of LLMs.

Our contributions can be summarized as follows.

- We propose the COD framework to address high variance and emergent phenomena in LLM performance scaling by effectively modeling the difficulty distribution within the evaluation sets.
- We introduce a performance scaling law for cluster-wise performance prediction, with theoretical support and experimental validation.
- Extensive experiments conducted in eight different evaluation sets demonstrate that COD provides reliable predictions with an average prediction error of 1.36% on an LLM with 70B parameters.

2 Related Work

2.1 Loss Scaling Laws

Loss scaling laws provide a systematic framework for understanding the relationship between computational resources, data, model size, and the LLM performance. Early work by Kaplan et al. [25] demonstrates that the pre-training loss of LLMs follows a power-law relationship with the compute (the number of floating-point operations) used in training. Subsequent studies extend these findings to other domains, such as computer vision [47], graph learning [30], and vision-language models [3, 20]. Recent research has also explored scaling laws in specific contexts, such as fine-tuning [21, 40], vocabulary size optimization [39], retrieval-augmented models [34], and hyperparameter tuning [27, 46]. These studies highlight the broad applicability of scaling laws and their potential to guide the efficient allocation of computational resources.

2.2 Downstream Task Performance Scaling

Predicting downstream task performance remains a critical challenge due to emergent abilities in LLMs that some capabilities manifest only after exceeding task-specific thresholds [32, 42]. Recent works, such as using loss as a proxy [8] or increasing metric resolution [23], have demonstrated potential but encounter challenges in aligning surrogate metrics with original task objectives. Here, we briefly review the two main types of methods for predicting downstream performance:

Loss-intermediate prediction. These methods predict the final training loss (or in-domain validation loss) of LLMs with loss scaling laws first, and then predict downstream performance through loss-performance relationships [8, 11, 16]. While these methods leverage established scaling laws for loss predictions, they encounter a fundamental limitation: the inconsistent mapping between loss and performance metrics. In addition, Xiao et al. [43] employ the evaluation set answer loss as an intermediate variable for estimation.

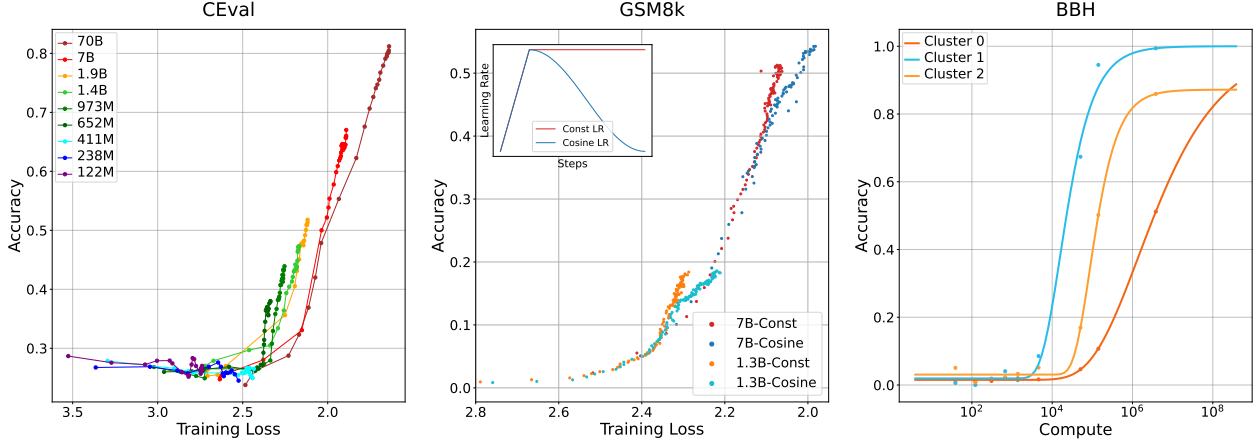


Figure 1 Performance-loss relationship across different model sizes (left) and learning rate schedules (middle). Performance-compute relationship for different clusters of the BBH samples (right)

Although answer loss correlates with the final performance metrics, its predictability remains low as predicting answer loss shares the challenges with predicting performance, including emergence phenomenon and high variance in task difficulty.

End-to-end performance-compute prediction. These methods [1, 7, 23, 31] directly model the relationship between performance and the compute budget (or the number of model parameters). Specifically, Achiam et al. [1] estimate and fit this relationship using a subset of the evaluation set, while still failing to predict the full set. Hu et al. [23] address the challenge of non-emergent capabilities in smaller models by employing multiple non-greedy decoding evaluations, thereby enabling accurate extrapolation of performance predictions for models with up to 2.4B parameters. Caballero et al. [7] propose a smooth broken power-law that models LLM scaling by decomposing it into multi-segment power laws. However, when predicting metrics for large-scale models (e.g., 70B parameters), performance trends often exhibit unexpected inflection points due to emergent capabilities or saturation effects, making piecewise functions inadequate for capturing these novel scaling regimes.

3 Pilot Study

In this section, we present the pilot experiments to illustrate the shortcomings of existing approaches.

Training loss may mismatch downstream task performance. Predicting downstream performance from training loss assumes LLMs achieve identical downstream results at the same loss value, which does not hold universally. In practice, training loss primarily serves as an indicator of in-domain fitting, whereas downstream tasks typically represent out-of-domain evaluations. Moreover, training configurations, such as model size and learning rate, can significantly affect not only the final loss but also the model’s generalization capabilities.

figure 1(left) illustrates the performance-loss relationships for LLMs of different sizes on the CEval benchmark [33]. At the same training loss level, smaller models can outperform larger ones in terms of test accuracy. Because smaller models initially exhibit weaker in-domain fitting capacity, they typically require more training steps to reach the same loss value, which can lead to better in-domain generalization once they do. figure 1(middle) compares the performance of LLMs trained under different learning rate schedules on the GSM8k dataset [9]. At the same loss level, the performance under the cosine schedule is always worse than that under the constant schedule, indicating that a lower learning rate may prioritize memorization over generalization, thereby diminishing downstream performance.

Diverse scaling patterns within the evaluation set. Different task samples exhibit unique computational thresholds, learning slopes, and upper bounds, making it challenging to find a single fitting function (or function group) that generalizes well across diverse task samples. figure 1(right) illustrates the performance-

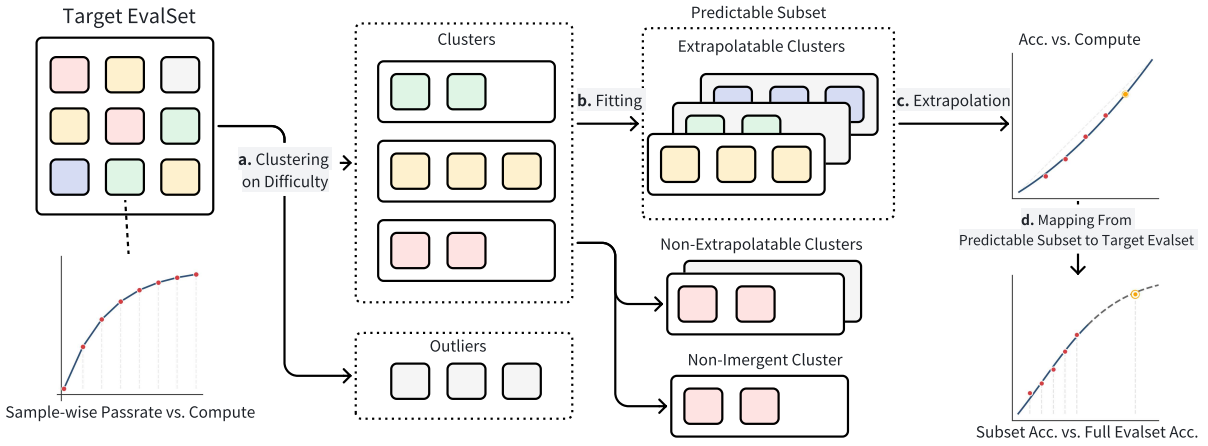


Figure 2 The pipeline of Cluster-On-Difficulty downstream task performance scaling, including 4 stages: **a.** Represent task difficulty feature with task-wise passrate vector. Cluster on the difficulty feature and filter outliers. **b.** Fit cluster-wise performance-compute curve. Classify clusters into extrapolatable clusters, non-extrapolatable clusters, and non-emergent clusters. **c.** Predict accuracy on extrapolatable clusters. **d.** Map subset accuracy prediction to full evaluation set performance.

compute relationships on three random clusters of the BBH benchmark [38], with each cluster containing samples with similar difficulty. Even within a single evaluation set, these scaling curves can vary significantly, indicating that a one-size-fits-all performance-compute curve is insufficient for capturing the full spectrum of a downstream evaluation set.

Taken together, these observations highlight the importance of modeling the heterogeneous scaling properties within an evaluation set and identifying a robust intermediate metric to serve as a reliable indicator of the downstream performance of LLMs.

4 Method

In this section, we first introduce the problem formulation. Then we present the COD method in four parts, as illustrated in figure 2: 1) We show the construction of sample-level difficulty scaling feature and present an improved mean-shift clustering algorithm (Sec. 4.1); 2) We derive a performance scaling law corresponding to task difficulty variance, which supports extrapolating the performance-compute relationship for task clusters with similar difficulty features (Sec. 4.2). We fit cluster-wise performance-compute curves on small models and filter extrapolatable clusters; 3) We extrapolate the performance on extrapolatable clusters and predict the accuracy of the target large model on the predictable subset (Sec. 4.3); 4) We show how to map accuracy on the predictable subset to full evaluations (Sec. 4.4).

Problem Formulation. Consider a language model M_C trained with a compute budget of C measured in FLOPs. Let \mathcal{P} be a set of downstream tasks that we aim to evaluate the model on. Each sample $T \in \mathcal{P}$ is defined by a question-answer pair (q, a_{true}) . Given a question q , the model M_C outputs a probability distribution $p(a|q; M_C)$ over the space of all possible answers.

Our goal is to predict the downstream task performance of a large language model $M_{C_{\text{target}}}$ using only evaluation results from smaller models $\{M_{C_1}, M_{C_2}, \dots, M_{C_n}\}$ where $C_i \ll C_{\text{target}}$ for all i . Formally, we aim to found the prediction method ϕ to minimize the absolute prediction error over a group of tasks sets $\{\mathcal{P}_j\}_m$:

$$\arg \min_{\phi} \frac{1}{m} \sum_{i=1}^m \frac{1}{|\mathcal{P}_j|} \sum_{T \in \mathcal{P}_j} |\widehat{\text{Acc}}(C_{\text{target}}, T) - \text{Acc}(C_{\text{target}})|,$$

$$\widehat{\text{Acc}}(C_{\text{target}}, T) := \phi(\{\text{Acc}(C_i, T)\}_{i=1}^n, \{C_i\}_{i=1}^n, C_{\text{target}}),$$

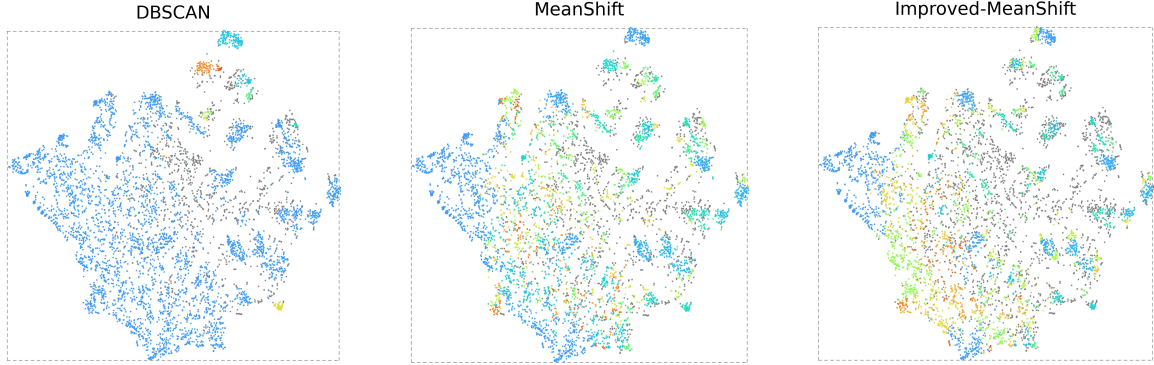


Figure 3 t-SNE visualization of different clustering methods: DBSCAN(left), MeanShift(Middle), Improved-MeanShift(Right). Each point represents an evaluation sample.

where $\text{Acc}(C, T)$ denotes the accuracy of model M_C on task T , and $\widehat{\text{Acc}}(C_{\text{target}}, T)$ is the predicted accuracy for the target model.

4.1 Clustering on Difficulty

Tasks within evaluation sets, despite common themes, show substantial difficulty differences, leading to diverse scaling patterns that hinder universal fitting functions. We propose clustering tasks by similar performance scaling behaviors to minimize intra-cluster heterogeneity while ensuring robust evaluation with sufficient samples per cluster.

Specifically, we train a group of language models with increasing parameter counts. These models are trained with the same ratio of training tokens to compute per token. For each task, we generate 100 samples using `top_p=0.7` and `temperature=1.0` for each model, and compute the pass rate by averaging the results. This pass rate serves as an estimate of the model’s expected accuracy on the task. The resulting values are organized into a difficulty vector, ordered by increasing model size. For most tasks, this difficulty vector exhibits a monotonic increase, reflecting the gradual improvement of model capability with scale.

After obtaining the difficulty feature vector for each task, we use the improved clustering algorithm that incorporates the following features: (1) Minimizing intra-class variance to ensure similar extrapolation properties within each cluster; (2) Automatic determination of cluster numbers, as the optimal number varies across evaluation sets and is difficult to pre-specify.

To further reduce intra-class variance, we propose an improved MeanShift algorithm to constrain the cluster diameter. At the same time, we maintain a minimum number of tasks in each cluster to reduce metric fluctuations. We provide the t-SNE visualization of clustering results evaluation tasks on BBH [38] to compare the proposed method and classic clustering algorithms including DBSCAN [14] and MeanShift [15]. Each point represents an evaluation sample, and its color denotes the cluster type. As shown in figure 3, our improved MeanShift effectively splits dense areas whereas DBSCAN and the original MeanShift produce connected clusters with large within-cluster distances.

We provide numerical comparison of clustering algorithms in Sec. 5.3.1 and explain implementation details of imporved MeanShift in Appendix A.1, smoothing techniques in Appendix A.2.

4.2 Fitting

After clustering, we compute metrics for small models within each cluster. We then apply a novel performance scaling law, based on theoretical analysis, to fit accuracy-to-compute curves for each cluster, focusing on clustered samples after excluding outliers. We derive the following fitting formula for the downstream task scaling law based on the training loss scaling law.

Theorem 1 (Scaling Law for Downstream Task Performance). *Consider a language model M_C trained with compute budget C and a set of downstream tasks \mathcal{P} . Under the following assumptions: Assumption 1 (Power-law scaling of answer loss): the expected answer loss follows:*

$$L_{\mathcal{P}}(C) := \mathbb{E}_{(q, a_{true}) \sim \mathcal{P}}[L(q, a_{true}; C)] = \alpha C^{-\beta} + \gamma \quad (1)$$

where $\alpha, \beta, \gamma > 0$ are task-specific constants, with γ representing the irreducible loss.

Assumption 2 (Unique deterministic answers): Each question has a unique deterministic answer. The model receives score 1 if and only if M_C outputs a_{true} , and 0 otherwise.

Assumption 3 (Accuracy decomposition): The expected accuracy decomposes as:

$$\mathbb{E}_{T \sim \mathcal{P}}[\text{Acc}(C)] = g + (1 - g) \cdot \mathbb{E}_{(q, a_{true}) \sim \mathcal{P}}[p(a_{true} | q, M_C)], \quad (2)$$

where $g \in [0, 1]$ is the random guessing baseline.

Then, the expected accuracy on task set \mathcal{P} can be modeled as:

$$\mathbb{E}_{\mathcal{P}}[\text{Acc}(C)] = g + (1 - g) \left(\exp(-\alpha C^{-\beta} - \gamma) + \frac{\sigma_L^2(C)}{2\mu_L(C)} \right) + o(\sigma_L^2(C)) \quad (3)$$

where $\mu_L(C) = \mathbb{E}_{(q, a_{true}) \sim \mathcal{P}}[L(q, a_{true}; C)]$ is the mean loss and $\sigma_L^2(C) = \text{Var}_{(q, a_{true}) \sim \mathcal{P}}[L(q, a_{true}; C)]$ is the loss variance across the task set.

Proof Sketch. By definition of the language model loss, $p(a_{true} | q, M_C) = \exp(-L(q, a_{true}; C))$. Under Assumption 1, if the answer loss follows a power law $L \sim \alpha C^{-\beta} + \gamma$, then the task passrate should approximately scale as $\exp(-\alpha C^{-\beta} - \gamma)$.

The key subtlety lies in the averaging: accuracy computes $\mathbb{E}[\exp(-L)]$ (arithmetic mean of passrates) while the loss scaling law gives us $\exp(-\mathbb{E}[L])$ (geometric mean). Using Taylor expansion:

$$\mathbb{E}[\exp(-L)] \approx \exp(-\mu_L) + \frac{\sigma_L^2}{2\mu_L}$$

where μ_L and σ_L^2 are the mean and variance of the loss distribution.

This approximation is accurate when tasks have similar difficulty feature ($\sigma_L^2/\mu_L^2 \ll 1$), motivating our clustering approach to reduce intra-cluster variance. Assumption 3 adds the parameter g for random guessing. The complete proofs are provided in Appendix B. \square

[Theorem 1](#) demonstrates that a metric of an evaluation set with similar difficulty features can be effectively modeled using the following formula:

$$y(C) = g + (1 - g) * e^{-aC^{-b} - c}, \quad (4)$$

where a and b jointly influence how accuracy varies with C , c controls the upper bound of the fitting curve, and g represents the expected random guess metric for a task cluster. a, b, c , and g are trainable parameters. Note that these assumptions may not perfectly hold in practice, we provide additional discussions on assumption 3 in Appendix I.

4.3 Extrapolation

To ensure reliable extrapolation, we identify clusters exhibiting robust scaling patterns, as some clusters may show saturated or non-emergent performance on smaller models, making them unsuitable for prediction. We aim to find an extrapolation subsets that represent the full set performance, and use the subset metric as an intermediate indicator for the prediction of the full set accuracy.

A cluster is deemed **extrapolatable** if it meets two criteria: (1) its expected accuracy increases monotonically with model size, and (2) its performance converges to at least a predefined threshold P (where $P \leq 1$ accounts for practical limits like ambiguous questions or finite training coverage).

We filter out non-extrapolatable clusters using two rules based on the parameters from Eq. (4):

1. Negligible accuracy growth, indicated by minimal a or b values.
2. Poor extrapolation reliability, indicated by an excessive c value.

In practice, for extrapolatable clusters, we set $a > 1$, $b > 0.1$, and $0 \leq c < 1$. Further ablation experiments are provided in Appendix C.1.

The clusters satisfying these conditions form the *predictable subset*. The final performance prediction for a target model on this subset is the weighted average of the extrapolated predictions from these individual clusters, with weights proportional to cluster sizes.

4.4 Mapping from Predictable Subset to Target Evaluation Set

We map predictions from the predictable subset \mathcal{P}' to the complete evaluation set \mathcal{P} using a function g . This approach is based on the observation that extrapolatable and non-extrapolatable samples, while differing in difficulty, often share question types, suggesting a preserved relative metric ordering. The mapping function $f : \text{Acc}(\mathcal{P}') \rightarrow \text{Acc}(\mathcal{P})$ is continuous, smooth over $[0, 1]$, monotonically increasing, and constrained to pass through $(0, 0)$ and $(1, 1)$. Empirical validation indicates a polynomial function optimally captures this relationship:

$$f_n(x) = \alpha_{n-1}x^n + \alpha_{n-2}x^{n-1} + \dots + \alpha_1x^2 + (1 - \alpha_1 - \alpha_2 - \dots - \alpha_{n-1})x, \quad (5)$$

where x represents the average accuracy of the predictable subset \mathcal{P}' , and n denotes the highest degree of the polynomial. In practical implementation, a quartic function is employed to fit the mapping (see Appendix C.2 for exhaustive experimental details). To ensure reliability, we calibrate f using evaluation results from existing models as anchors. This subset-to-full mapping generally demonstrates robustness across diverse model architectures and training data, often permitting the use of external models (e.g., Qwen2-72B [45]) as anchors for many tasks (see Appendix C.3 for experiments). However, for data-sensitive tasks, models with similar training distributions provide more reliable anchors, prioritizing data consistency for mapping accuracy. The final metric prediction for a target LLM with estimated training computation C_0 is then $p = f \circ y(C_0)$, combining the cluster-wise extrapolation $y(C_0)$ from Eq. (4) with the mapping f .

5 Experiments

5.1 Experimental Setups

In our experimental setup, we train nine language models ranging from 122M to 70B parameters in total, which share the same data distribution and architecture, with the training data scaled proportionally to their sizes. We show the detailed training configurations and recip in Appendix D.

For evaluation, we adopt the following widely used benchmarks, including GSM8K [9], MATH [19], BBH [38], TriviaQA [24], MBPP [4], AGIEval [50], DROP [12], MMLU-pro [41]. All models are evaluated in a few-shot in-context learning manner, and we aligned our evaluation setups with LLaMa3 [13]. We evaluate our proposed COD performance scaling for LLMs against existing approaches on multiple public benchmarks. Using eight smaller language models as known information, we estimate the downstream task performance of a pretrained LLM with 70B parameters.

5.2 Prediction Experiments

We compare COD against four representative prediction methods:

1. Loss-intermediate performance prediction [8]: First predicts the target LLM’s final training loss, then estimates downstream task metrics based on the relationship between smaller models’ evaluation metrics and their losses.

Table 1 Absolute prediction error (%) on evaluation sets for predicting the performance of the 70B model. Errors $< 2\%$ are considered accurate (green), while errors $> 5\%$ are considered invalid (red). \downarrow indicates lower is better.

Method	Overall Metrics		Individual Task Sets							
	Mean \downarrow	Max \downarrow	GSM8k	MATH	BBH	TriviaQA	MBPP	AGIEval	DROP	MMLU-pro
Loss-intermediate	5.29	9.39	9.39	6.95	2.33	5.81	5.52	1.41	5.37	5.55
End-to-end	3.10	6.00	4.00	3.86	0.64	0.68	1.75	6.00	4.11	3.72
Passrate	5.02	8.80	6.71	8.80	3.51	4.00	7.34	6.78	0.26	2.74
BNSL	5.17	13.05	4.23	5.88	13.05	5.86	2.55	0.82	1.53	7.42
COD (w/o mapping)	2.24	5.26	4.70	0.50	2.91	1.98	0.89	5.26	1.08	0.57
COD (Complete)	1.63	2.38	2.23	1.28	1.77	1.64	2.19	2.38	0.23	1.35

2. End-to-end performance-compute prediction: Directly extrapolates large model metrics from smaller model evaluation set metrics using performance scaling laws [43].
3. Passrate-compute prediction [1, 23]: A variant of end-to-end method, which estimates large model passrates from smaller model passrates. We conduct 100 trials per evaluation set for smaller models to enhance reliability and report absolute prediction error on the passrate metric.
4. BNSL [7]: Another variant of end-to-end method, which decomposes the end-to-end mapping into a multi-segment power-law framework.

We also evaluate two variants of our COD approach to validate the benefits of its components:

1. COD (w/o mapping): Employs difficulty-based clustering, extrapolates within all clusters, and aggregates metrics, bypassing the subset-to-full mapping stage.
2. COD (Complete): Our full proposed multi-stage approach, including clustering, predictable cluster filtering, subset extrapolation, and subset-to-full mapping.

Comparative results are shown in Tab. 1. Prediction accuracy is measured by the absolute error between predicted and actual performance. We report mean and max prediction errors across all evaluation sets, as well as errors for individual sets. Our complete COD approach significantly outperforms existing methods in both mean (1.68%) and maximum (2.38%) prediction errors, offering reliable guidance for large model training. While baselines perform well on some sets, their substantial errors on others undermine overall credibility.

figure 4 visualizes the performance-compute relationships. The COD method does not merely extend the existing scaling trend; instead, it effectively predicts whether growth slowdown will occur subsequently and enables better estimation of the magnitude of curve bending. On BBH, while all methods give similar final estimates, end-to-end and loss-intermediate methods fit small model data poorly. COD reveals a more complex, better-fitted multi-phase trajectory. On MATH and MMLU-pro, where predicting accelerated growth versus plateaus is crucial, the loss-intermediate method underestimates model ceilings, and the end-to-end method exceeds 3% error. COD’s superior performance stems from its nuanced analysis of difficulty distributions and scaling laws, allowing it to predict growth in challenging sets and capture diminishing returns in saturated sets.

To further validate the generalizability of the COD method, we examine its predictive capabilities across different model scales and for models after continual training. In addition to the 70B model, the COD method also demonstrates effectiveness in predicting the capabilities of the medium-size models, with experimental details and corresponding conclusions available in Appendix E. Beyond this, the method is further shown to be capable of predicting the performance of LLMs following a continual training phase on high-quality data. To validate this, we conducted dedicated experiments and in-depth analyses on continually trained LLMs, with results documented in Appendix F.

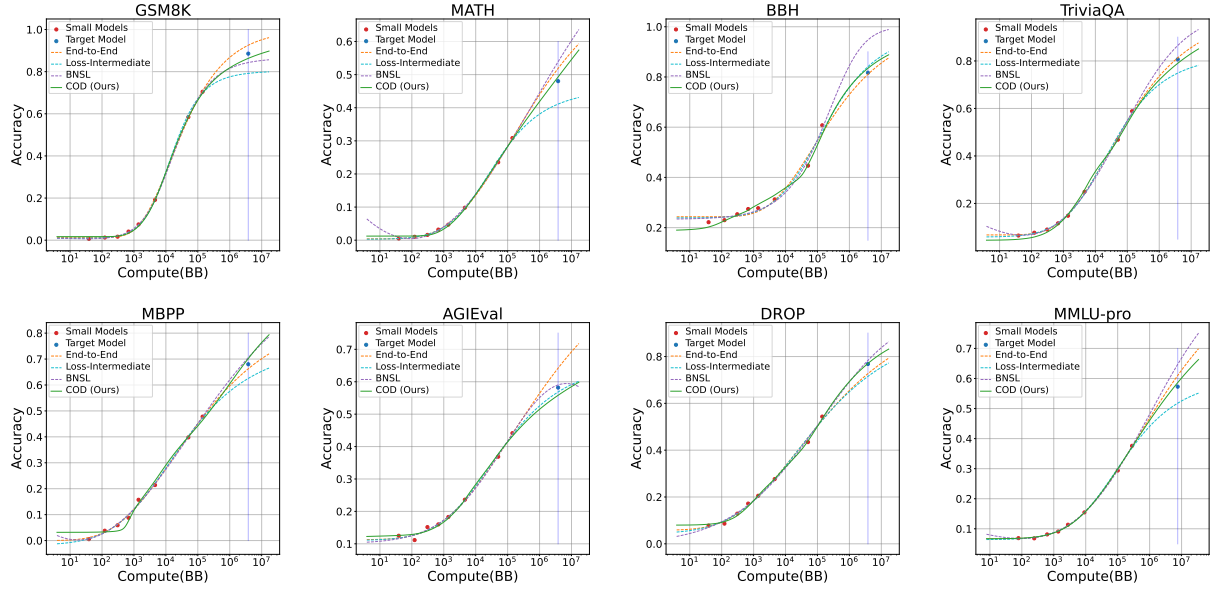


Figure 4 Performance-compute relationship for different prediction methods on eight evaluation sets.

5.3 Ablation Study

In this section, we conduct ablation experiments on the clustering method and extrapolation function, while in the Appendix C we discuss ablation studies on the selection criteria for extrapolatable subsets, interpolation mapping methods, and the impact of anchor point selection on predictions.

5.3.1 Comparison of Clustering Methods

We assess the impact of different clustering algorithms on prediction accuracy. The goal is to achieve tight intra-cluster difficulty similarity (low average distance to center) while maintaining cluster stability (min. 10 samples/cluster). We compare our Improved-MeanShift with DBScan, MeanShift, and K-Means. For K-Means, we adjust it to approximate our goals: (1) search for k yielding min. cluster sizes ≈ 10 ; (2) treat samples outside a radius (e.g., $2 \times$ average intra-cluster distance) from any cluster center as outliers, ensuring clusters don't drop below 10 samples. We term this "Improved-KMeans" for this comparison. Clustering quality is measured by Intra-cluster Average Distance (IAD) and Outlier Rate (OR). Prediction benefits are measured by Extrapolation Error (EE) on the predictable subset and Final prediction Error (FE) on the full evalset. (Tab. 2).

Tab. 2 shows Improved-KMeans and Improved-MeanShift yield better clustering (lower IAD) due to their intra-cluster distance constraints. The results also confirm these methods lead to lower EE and FE. Although Improved-KMeans has the best IAD, its GSM8k prediction is poor. This is likely because K-Means requires pre-specifying k , and our search for k can be unstable, leading to large errors on some sets. In contrast, our Improved-MeanShift, which automatically determines k based on distance constraints, offers more stable clustering and the lowest maximum prediction error.

5.3.2 Different Extrapolation Formulas

We ablate our proposed fitting formula $f(C) = g + (1 - g) \cdot e^{-aC^{-b} - c}$ (Ours) by removing or modifying components: (1) $f_1(C) = e^{-aC^{-b} - c}$ (w/o random guess); (2) $f_2(C) = g + (1 - g) \cdot e^{-aC^{-b}}$ (w/o constant c); (3) $f_3(C) = e^{-aC^{-b}}$ (Direct Power Law [23]). Tab. 3 shows Extrapolation Error (EE), Task Ratio of predictable subset (TR), and Final prediction Error (FE). Our proposed formula f consistently achieves the lowest EE and FE. f_1 struggles with finite-answer tasks where small models have non-zero scores. f_2

Table 2 Clustering performance across different algorithms on metrics including IAD (Intra-cluster Average Distance \downarrow), OR (Outlier Rate %), EE (Extrapolation Error \downarrow), FE (Final Prediction Error \downarrow). The bottom lines show the mean and max EE and FE across evalsets.

Dataset	K-Means				DBScan				MeanShift				Improved-KMeans				Improved-MeanShift			
	IAD	OR	EE	FE	IAD	OR	EE	FE	IAD	OR	EE	FE	IAD	OR	EE	FE	IAD	OR	EE	FE
MMLU-pro	0.32	-	3.69	3.69	0.42	0.56	3.72	3.69	0.29	0.39	3.15	3.08	0.16	2.85	0.56	0.61	0.22	4.40	1.27	1.35
GSM8k	0.22	-	0.01	0.00	0.51	0.53	4.08	4.12	0.29	0.61	0.67	0.74	0.13	2.73	3.92	4.08	0.19	4.93	2.20	2.23
MATH	0.22	-	2.62	2.34	0.48	0.68	4.38	4.16	0.21	1.44	2.55	2.26	0.09	2.22	0.81	0.51	0.15	2.66	1.14	1.28
BBH	0.63	-	8.16	8.99	0.71	18.92	3.53	4.36	0.27	20.72	2.12	0.65	0.20	37.23	0.02	2.17	0.21	33.58	0.29	1.77
TriviaQA	0.44	-	2.97	2.46	0.70	6.38	1.11	0.81	0.25	6.77	3.64	4.90	0.12	11.97	1.18	1.12	0.19	11.54	1.58	1.64
AGIEval	0.46	-	2.61	2.68	0.56	3.67	6.43	6.27	0.29	2.99	2.63	3.23	0.15	7.60	5.96	5.56	0.21	11.50	1.11	2.38
DROP	0.56	-	1.66	1.64	0.67	11.08	3.03	2.66	0.25	11.81	4.18	4.00	0.14	21.42	3.99	5.24	0.20	19.88	0.26	0.23
MBPP	0.34	-	2.53	2.67	0.51	12.80	1.57	1.41	0.22	15.60	2.40	1.22	0.17	19.40	2.39	3.25	0.17	21.60	1.56	2.19
Mean	-	-	3.62	3.76	-	-	3.93	4.08	-	-	2.12	1.68	-	-	1.33	1.84	-	-	1.23	1.66
Max	-	-	8.16	8.99	-	-	4.38	4.36	-	-	3.15	3.08	-	-	3.92	4.08	-	-	2.20	2.23

Table 3 Ablation study on extrapolation formulas. EE, TR, FE shown for BBH, MATH, MMLU-pro.

Method	BBH			MATH			MMLU-pro		
	EE \downarrow	TR(%)	FE \downarrow	EE \downarrow	TR(%)	FE \downarrow	EE \downarrow	TR(%)	FE \downarrow
Direct Power Law (f_3)	8.90	49.06	8.88	3.81	81.46	3.35	4.30	95.15	4.27
w/o Random Guess (f_1)	10.27	45.75	11.20	4.04	81.46	3.55	4.40	95.05	4.37
w/o Constant c (f_2)	2.14	57.26	4.01	1.40	81.46	1.56	3.85	95.60	3.88
Ours (f)	0.29	52.46	1.77	1.14	81.24	1.28	1.27	94.38	1.35

inaccurately assumes perfect scores are attainable, ignoring data limitations and task ambiguities. The direct power law (f_3) fails to model the 0-1 metric range and the varying difficulty of improvement near random guess and saturation. TR’s minor influence on prediction error suggests robustness; even with low TR due to non-emergent tasks, their performance can be largely predicted via mapping.

6 Conclusion and Discussion

In this work, we introduce a novel downstream performance scaling framework including (1) the COD method that effectively models the underlying diverse scaling patterns of evaluation tasks; (2) a scaling law for downstream task performance that provides a fitting formula for performance-compute extrapolation; and (3) a systematic methodology for identifying and leveraging predictable subset that provides a robust intermediate metric for accurate full-set performance predictions. We discuss the limitations and future works in Appendix I.

Ethics Statement

We have read and adhered to the ICLR Code of Ethics. This work proposes a computational framework to enable more efficient resource allocation in the training of LLMs. The research is methodological in nature and aims to support more sustainable and responsible practices within the field of AI development.

We provide a detailed account of our methods, theoretical proofs, and experimental settings. We openly discuss the limitations of our framework in Appendix I. This study does not involve human subjects or the use of sensitive personal data.

We utilized language models at the writing level, including checking for grammatical errors in the article and modifying expressions. The use of language models had no impact on the article’s innovative contributions, experiments, or analytical perspectives.

Reproducibility Statement

We have made extensive efforts to ensure the reproducibility of our work. The core methodology, the Clustering-On-Difficulty (COD) framework, is detailed in Sec. 4. The improved MeanShift clustering algorithm is described in Sec. 4.1, with full pseudocode provided in Appendix A.1 (Algorithm 1). Our performance scaling law (Theorem 1) is presented in Sec. 4.2, with a complete proof available in Sec. B. We discuss the additional computational cost of the COD method in Appendix H.

Our experimental setup, including model architectures, training data philosophy, and hyperparameters, is thoroughly documented in Sec. 5.1 and Appendix D, with specific model configurations listed in Tab. A4. The evaluation benchmarks, protocols, and few-shot settings are described in Sec. 5.1 and summarized in Tab. A5. Extensive ablation studies validating our component choices—including extrapolation formulas (Sec. 5.3.2), clustering algorithms (Appendix 5.3.1), interpolation methods (Appendix C.2), and criteria for filtering clusters (Appendix C.1)—are provided to support our findings. We visualize the task difficulty distribution for each evalset in Appendix G.

References

- [1] Josh Achiam, Steven Adler, Sandhini Agarwal, Lama Ahmad, Ilge Akkaya, Florencia Leoni Aleman, Diogo Almeida, Janko Altenschmidt, Sam Altman, Shyamal Anadkat, et al. Gpt-4 technical report. [arXiv preprint arXiv:2303.08774](#), 2023.
- [2] Joshua Ainslie, James Lee-Thorp, Michiel De Jong, Yury Zemlyanskiy, Federico Lebrón, and Sumit Sanghai. Gqa: Training generalized multi-query transformer models from multi-head checkpoints. [arXiv preprint arXiv:2305.13245](#), 2023.
- [3] Ibrahim M Alabdulmohsin, Behnam Neyshabur, and Xiaohua Zhai. Revisiting neural scaling laws in language and vision. *Adv. Neural Inform. Process. (NeurIPS)*, 35:22300–22312, 2022.
- [4] Jacob Austin, Augustus Odena, Maxwell Nye, Maarten Bosma, Henryk Michalewski, David Dohan, Ellen Jiang, Carrie Cai, Michael Terry, Quoc Le, et al. Program synthesis with large language models. [arXiv preprint arXiv:2108.07732](#), 2021.
- [5] Hritik Bansal, Arian Hosseini, Rishabh Agarwal, Vinh Q Tran, and Mehran Kazemi. Smaller, weaker, yet better: Training llm reasoners via compute-optimal sampling. In *The 4th Workshop on Mathematical Reasoning and AI at NeurIPS*, 2024.
- [6] Sébastien Bubeck, Varun Chandrasekaran, Ronen Eldan, Johannes Gehrke, Eric Horvitz, Ece Kamar, Peter Lee, Yin Tat Lee, Yuanzhi Li, Scott Lundberg, et al. Sparks of artificial general intelligence: Early experiments with gpt-4. [arXiv preprint arXiv:2303.12712](#), 2023.
- [7] Ethan Caballero, Kshitij Gupta, Irina Rish, and David Krueger. Broken neural scaling laws. [arXiv preprint arXiv:2210.14891](#), 2022.
- [8] Yangyi Chen, Binxuan Huang, Yifan Gao, Zhengyang Wang, Jingfeng Yang, and Heng Ji. Scaling laws for predicting downstream performance in llms. [arXiv preprint arXiv:2410.08527](#), 2024.
- [9] Karl Cobbe, Vineet Kosaraju, Mohammad Bavarian, Mark Chen, Heewoo Jun, Lukasz Kaiser, Matthias Plappert, Jerry Tworek, Jacob Hilton, Reiichiro Nakano, et al. Training verifiers to solve math word problems. [arXiv preprint arXiv:2110.14168](#), 2021.
- [10] DeepSeek-AI et al. Deepseek-v3 technical report, 2025. URL <https://arxiv.org/abs/2412.19437>.
- [11] Zhengxiao Du, Aohan Zeng, Yuxiao Dong, and Jie Tang. Understanding emergent abilities of language models from the loss perspective. [arXiv preprint arXiv:2403.15796](#), 2024.
- [12] Dheeru Dua, Yizhong Wang, Pradeep Dasigi, Gabriel Stanovsky, Sameer Singh, and Matt Gardner. DROP: A reading comprehension benchmark requiring discrete reasoning over paragraphs. In *NAACL-HLT*, pages 2368–2378, 2019.
- [13] Abhimanyu Dubey, Abhinav Jauhri, Abhinav Pandey, Abhishek Kadian, Ahmad Al-Dahle, Aiesha Letman, Akhil Mathur, Alan Schelten, Amy Yang, Angela Fan, et al. The llama 3 herd of models. [arXiv preprint arXiv:2407.21783](#), 2024.

[14] Martin Ester, Hans-Peter Kriegel, Jörg Sander, Xiaowei Xu, et al. A density-based algorithm for discovering clusters in large spatial databases with noise. In *KDD*, volume 96, pages 226–231, 1996.

[15] Keinosuke Fukunaga and Larry Hostetler. The estimation of the gradient of a density function, with applications in pattern recognition. *IEEE Transactions on information theory*, 21(1):32–40, 1975.

[16] Samir Yitzhak Gadre, Georgios Smyrnis, Vaishaal Shankar, Suchin Gururangan, Mitchell Wortsman, Rulin Shao, Jean Mercat, Alex Fang, Jeffrey Li, Sedrick Keh, et al. Language models scale reliably with over-training and on downstream tasks. *arXiv preprint arXiv:2403.08540*, 2024.

[17] Aaron Grattafiori, Abhimanyu Dubey, Abhinav Jauhri, Abhinav Pandey, Abhishek Kadian, Ahmad Al-Dahle, Aiesha Letman, Akhil Mathur, Alan Schelten, Alex Vaughan, et al. The llama 3 herd of models. *arXiv preprint arXiv:2407.21783*, 2024.

[18] Daya Guo, Dejian Yang, Haowei Zhang, Junxiao Song, Ruoyu Zhang, Runxin Xu, Qihao Zhu, Shirong Ma, Peiyi Wang, Xiao Bi, et al. Deepseek-r1: Incentivizing reasoning capability in llms via reinforcement learning. *arXiv preprint arXiv:2501.12948*, 2025.

[19] Dan Hendrycks, Collin Burns, Saurav Kadavath, Akul Arora, Steven Basart, Eric Tang, Dawn Song, and Jacob Steinhardt. Measuring mathematical problem solving with the MATH dataset. In *Adv. Neural Inform. Process. Syst. (NeurIPS)*, 2021.

[20] Tom Henighan, Jared Kaplan, Maxwell Katz, Anselm Levskaya, Sam McCandlish, Andreas Stuhlmuller, Scott Gray, and Dario Amodei. Scaling laws for autoregressive generative modeling. *arXiv preprint arXiv:2010.14701*, 2020.

[21] Danny Hernandez, Jared Kaplan, Tom Henighan, and Sam McCandlish. Scaling laws for transfer. *arXiv preprint arXiv:2102.01293*, 2021.

[22] Jordan Hoffmann, Sebastian Borgeaud, Arthur Mensch, Elena Buchatskaya, Trevor Cai, Eliza Rutherford, Diego de Las Casas, Lisa Anne Hendricks, Johannes Welbl, Aidan Clark, et al. Training compute-optimal large language models. *arXiv preprint arXiv:2203.15556*, 2022.

[23] Shengding Hu, Xin Liu, Xu Han, Xinrong Zhang, Chaoqun He, Weilin Zhao, Yankai Lin, Ning Ding, Zebin Ou, Guoyang Zeng, et al. Predicting emergent abilities with infinite resolution evaluation. In *Int. Conf. Learn. Rep. (ICLR)*, 2024.

[24] Mandar Joshi, Eunsol Choi, Daniel S Weld, and Luke Zettlemoyer. Triviaqa: A large scale distantly supervised challenge dataset for reading comprehension. In *Annual Meeting of the Association for Computational Linguistics*, pages 1601–1611, 2017.

[25] Jared Kaplan, Sam McCandlish, Tom Henighan, Tom B Brown, Benjamin Chess, Rewon Child, Scott Gray, Alec Radford, Jeffrey Wu, and Dario Amodei. Scaling laws for neural language models. *arXiv preprint arXiv:2001.08361*, 2020.

[26] Dmitry Lepikhin, HyoukJoong Lee, Yuanzhong Xu, Dehao Chen, Orhan Firat, Yanping Huang, Maxim Krikun, Noam Shazeer, and Zhifeng Chen. Gshard: Scaling giant models with conditional computation and automatic sharding. *arXiv preprint arXiv:2006.16668*, 2020.

[27] Lucas Lingle. A large-scale exploration of μ -transfer. *arXiv preprint arXiv:2404.05728*, 2024.

[28] Aixin Liu, Bei Feng, Bin Wang, Bingxuan Wang, Bo Liu, Chenggang Zhao, Chengqi Dengr, Chong Ruan, Damai Dai, Daya Guo, et al. Deepseek-v2: A strong, economical, and efficient mixture-of-experts language model. *arXiv preprint arXiv:2405.04434*, 2024.

[29] Anton Lozhkov, Loubna Ben Allal, Leandro von Werra, and Thomas Wolf. Fineweb-edu: the finest collection of educational content, 2024.

[30] Qian Ma, Haitao Mao, Jingzhe Liu, Zhehua Zhang, Chunlin Feng, Yu Song, Yihan Shao, and Yao Ma. Do neural scaling laws exist on graph self-supervised learning? *arXiv preprint arXiv:2408.11243*, 2024.

[31] David Owen. How predictable is language model benchmark performance? *arXiv preprint arXiv:2401.04757*, 2024.

[32] Rylan Schaeffer, Brando Miranda, and Sanmi Koyejo. Are emergent abilities of large language models a mirage? In *Adv. Neural Inform. Process. Syst. (NeurIPS)*, 2023.

[33] Christin Seifert, Jörg Schütterer, et al. Ceval: A benchmark for evaluating counterfactual text generation. In *International Natural Language Generation Conference*, pages 55–69, 2024.

[34] Rulin Shao, Jacqueline He, Akari Asai, Weijia Shi, Tim Dettmers, Sewon Min, Luke Zettlemoyer, and Pang Wei Koh. Scaling retrieval-based language models with a trillion-token datastore. [arXiv preprint arXiv:2407.12854](#), 2024.

[35] Noam Shazeer. Glu variants improve transformer. [arXiv preprint arXiv:2002.05202](#), 2020.

[36] Charlie Snell, Jaehoon Lee, Kelvin Xu, and Aviral Kumar. Scaling llm test-time compute optimally can be more effective than scaling model parameters. [arXiv preprint arXiv:2408.03314](#), 2024.

[37] Jianlin Su, Murtadha Ahmed, Yu Lu, Shengfeng Pan, Wen Bo, and Yunfeng Liu. Roformer: Enhanced transformer with rotary position embedding. *Neurocomputing*, 568:127063, 2024.

[38] Mirac Suzgun, Nathan Scales, Nathanael Schärli, Sebastian Gehrmann, Yi Tay, Hyung Won Chung, Aakanksha Chowdhery, Quoc Le, Ed Chi, Denny Zhou, et al. Challenging big-bench tasks and whether chain-of-thought can solve them. In *Findings of the Association for Computational Linguistics*, pages 13003–13051, 2023.

[39] Chaofan Tao, Qian Liu, Longxu Dou, Niklas Muennighoff, Zhongwei Wan, Ping Luo, Min Lin, and Ngai Wong. Scaling laws with vocabulary: Larger models deserve larger vocabularies. [arXiv preprint arXiv:2407.13623](#), 2024.

[40] Yi Tay, Mostafa Dehghani, Jinfeng Rao, William Fedus, Samira Abnar, Hyung Won Chung, Sharan Narang, Dani Yogatama, Ashish Vaswani, and Donald Metzler. Scale efficiently: Insights from pretraining and finetuning transformers. In *Int. Conf. Learn. Rep. (ICLR)*, 2022.

[41] Yubo Wang, Xueguang Ma, Ge Zhang, Yuansheng Ni, Abhranil Chandra, Shiguang Guo, Weiming Ren, Aaran Arulraj, Xuan He, Ziyan Jiang, et al. Mmlu-pro: A more robust and challenging multi-task language understanding benchmark. [arXiv preprint arXiv:2406.01574](#), 2024.

[42] Jason Wei, Yi Tay, Rishi Bommasani, et al. Emergent abilities of large language models. [arXiv preprint arXiv:2206.07682](#), 2022.

[43] Chaojun Xiao, Jie Cai, Weilin Zhao, Guoyang Zeng, Xu Han, Zhiyuan Liu, and Maosong Sun. Densing law of llms. [arXiv preprint arXiv:2412.04315](#), 2024.

[44] An Yang, Baosong Yang, Beichen Zhang, Binyuan Hui, Bo Zheng, Bowen Yu, Chengyuan Li, Dayiheng Liu, Fei Huang, Haoran Wei, Huan Lin, Jian Yang, Jianhong Tu, Jianwei Zhang, Jianxin Yang, Jiaxi Yang, Jingren Zhou, Junyang Lin, Kai Dang, Keming Lu, Keqin Bao, Kexin Yang, Le Yu, Mei Li, Mingfeng Xue, Pei Zhang, Qin Zhu, Rui Men, Runji Lin, Tianhao Li, Tingyu Xia, Xingzhang Ren, Xuancheng Ren, Yang Fan, Yang Su, Yichang Zhang, Yu Wan, Yuqiong Liu, Zeyu Cui, Zhenru Zhang, and Zihan Qiu. Qwen2.5 technical report. [arXiv preprint arXiv:2412.15115](#), 2024.

[45] An Yang, Baosong Yang, Beichen Zhang, Binyuan Hui, Bo Zheng, Bowen Yu, Chengyuan Li, Dayiheng Liu, Fei Huang, Haoran Wei, et al. Qwen2.5 technical report. [arXiv preprint arXiv:2412.15115](#), 2024.

[46] Greg Yang, Edward J Hu, Igor Babuschkin, Szymon Sidor, Xiaodong Liu, David Farhi, Nick Ryder, Jakub Pachocki, Weizhu Chen, and Jianfeng Gao. Tensor programs v: Tuning large neural networks via zero-shot hyperparameter transfer. [arXiv preprint arXiv:2203.03466](#), 2022.

[47] Xiaohua Zhai, Alexander Kolesnikov, Neil Houlsby, and Lucas Beyer. Scaling vision transformers. In *IEEE Conf. Comput. Vis. Pattern Recog. (CVPR)*, pages 1204–1213, 2022.

[48] Biao Zhang and Rico Sennrich. Root mean square layer normalization. *Advances in neural information processing systems*, 32, 2019.

[49] Chiyuan Zhang, Samy Bengio, Moritz Hardt, Benjamin Recht, and Oriol Vinyals. Understanding deep learning (still) requires rethinking generalization. *Communications of the ACM*, 64(3):107–115, 2021.

[50] Wanjun Zhong, Ruixiang Cui, Yiduo Guo, Yaobo Liang, Shuai Lu, Yanlin Wang, Amin Saied, Weizhu Chen, and Nan Duan. Agieval: A human-centric benchmark for evaluating foundation models. In *Findings of the Association for Computational Linguistics*, pages 2299–2314, 2024.

Contents

1	Introduction	1
2	Related Work	2
2.1	Loss Scaling Laws	2
2.2	Downstream Task Performance Scaling	2
3	Pilot Study	3
4	Method	4
4.1	Clustering on Difficulty	5
4.2	Fitting	5
4.3	Extrapolation	6
4.4	Mapping from Predictable Subset to Target Evaluation Set	7
5	Experiments	7
5.1	Experimental Setups	7
5.2	Prediction Experiments	7
5.3	Ablation Study	9
5.3.1	Comparison of Clustering Methods	9
5.3.2	Different Extrapolation Formulas	9
6	Conclusion and Discussion	10
A	Improvements of Clustering Algorithm	14
A.1	Improved MeanShift Algorithm	14
A.2	Smoothing Techniques	15
B	Proof of Theorem 1	16
C	Additional Ablation Studies	18
C.1	The Criteria for Extrapolatable Subsets	18
C.2	Interpolation Method	18
C.3	Different Anchor Points in Interpolation Mapping	19
D	Experimental Settings and Training Recipe	20
E	Additional Prediction Results for a Medium-size Model	21
F	Performance Prediction for Continue-Pretrained LLMs	21
G	Difficulty Distribution of Predictable Subset	22
H	Computational Cost	23
I	Limitations	23

A Improvements of Clustering Algorithm

A.1 Improved MeanShift Algorithm

We iteratively apply the MeanShift algorithm with a predefined cluster radius R and a minimum cluster size K . In each iteration, for the clustered samples, we examine whether the distance between each sample and its cluster center exceeds R , and relabel those samples that exceed this threshold as unclustered. For clusters containing fewer than K samples, we mark all samples in these clusters as unclustered. At the end of each iteration, we incorporate both the outliers from MeanShift and our marked unclustered samples into the next round of clustering, continuing this process until no further changes occur in sample labels. We present the pseudocode in [algorithm 1](#).

Algorithm 1 Iterative MeanShift Clustering Algorithm

```
1: Initialize all labels in the evaluation set to  $-1$ 
2: repeat
3:   Perform MeanShift clustering with radius  $R$  on all samples labeled  $-1$ 
4:   Assign new labels to clustered samples
5:   for each newly labeled sample  $i$  do
6:     Calculate distance  $dist_i$  to its cluster center
7:     if  $dist_i > R$  then
8:       Reset label to  $-1$ 
9:     end if
10:   end for
11:   for each cluster do
12:     if number of samples in cluster  $< K$  then
13:       Reset all samples in this cluster to  $-1$ 
14:     end if
15:   end for
16:   Renumber all non- $\{-1\}$  newly labeled samples to avoid overlap with old labels
17: until no label changes
```

In the experiment, K is empirically set to 10, which has been verified through extensive experiments to be a reasonable and robust value. The fixed radius R depends only on the value range and dimensionality (i.e., the number of predictive models) of the difficulty feature vectors. In our experiments, we fixed $R = 0.3$ for all evaluation sets to ensure consistent overall clustering performance. For experiments with different numbers of small models used for fitting, the value of R needs to be adaptively adjusted due to changes in the dimensionality of the feature vector. For instance, in the experiment of predicting the 12B-parameter model, R was empirically reduced from 0.3 to 0.2 to ensure that the intra-class error is reasonable.

Filtering zero-performance samples. In the evaluation set, there may exist a few extremely difficult problems that require sufficient model parameters to emerge. All small models may fail to solve these problems even after 100 evaluation attempts, resulting in difficulty feature vectors of all zeros. We refer to these as zero-performance samples. Their presence leads to two issues:

1. Zero performance on small models does not necessarily indicate zero accuracy on large models. For these samples, we cannot estimate when emergence will occur or predict large model metrics.
2. During clustering, they may be confused with other low-performing but non-zero samples. Including them in the same cluster would lower the expected accuracy of that cluster, leading to inaccurate fitting and extrapolation later.

Therefore, we pre-filter these zero-performance samples before clustering, treating them as outliers that do not participate in the clustering process. This approach obviates the necessity of considering their metrics under large models during subsequent extrapolation, and prevents disruption to the clustering of the remaining samples.

A.2 Smoothing Techniques

Metric fluctuations of individual samples in downstream tasks are not solely due to limited sampling. Another potential factor is noise from uneven data distribution in recent training batches. Therefore, in addition to performing 100 evaluations to mitigate sampling variance, we evaluated 100 times on each of the adjacent checkpoints before and after the selected model. We then averaged these accuracy expectation values across three checkpoints, further reducing sampling variance while offsetting noise from uneven training data distribution. This approach also reduces the number of zero-performance samples, further improving clustering and prediction effectiveness.

B Proof of Theorem 1

We use [lemma 1](#) to derive the scaling law for downstream task performance ([theorem 1](#)).

Lemma 1 (Arithmetic-geometric mean difference). *For any sequence of positive real numbers $\{x_i\}_{i=1}^n$, let:*

- $\mu_a = \frac{1}{n} \sum_{i=1}^n x_i$ be the arithmetic mean;
- $\mu_g = \prod_{i=1}^n x_i^{1/n}$ be the geometric mean;
- $\sigma^2 = \frac{1}{n} \sum_{i=1}^n (x_i - \mu)^2$ be the variance.

Then the difference between the arithmetic mean and geometric mean can be estimated as:

$$\Delta = \mu_a - \mu_g = \frac{1}{n} \sum_{i=1}^n x_i - \left(\prod_{i=1}^n x_i \right)^{\frac{1}{n}} = \frac{\sigma^2}{2\mu_a} + o(\sigma^2). \quad (6)$$

Proof. Taking the logarithm of the geometric mean μ_g :

$$\log(\mu_g) = \frac{1}{n} \sum_{i=1}^n \log x_i \quad (7)$$

Using Taylor expansion of $\log x$ around μ :

$$\log x = \log \mu + \frac{x - \mu}{\mu} - \frac{(x - \mu)^2}{2\mu^2} + o((x - \mu)^2). \quad (8)$$

We can simplify:

$$\begin{aligned} \frac{1}{n} \sum_{i=1}^n \log x_i &= \log \mu + \frac{1}{n} \sum_{i=1}^n \left(\frac{(x_i - \mu_a)}{\mu_a} - \frac{(x_i - \mu_a)^2}{2\mu_a^2} + o((x_i - \mu_a)^2) \right) \\ &= \log \mu + \underbrace{\frac{1}{\mu} \left(\frac{1}{n} \sum_{i=1}^n x_i - \mu_a \right)}_{\text{equal to 0}} + \underbrace{\frac{1}{2\mu_a^2} \left(\frac{1}{n} \sum_{i=1}^n (x_i - \mu_a)^2 \right)}_{\sigma^2} + o\left(\frac{1}{n} \sum_{i=1}^n (x_i - \mu_a)^2\right) \\ &= \log \mu - \frac{\sigma^2}{2\mu^2} + o(\sigma^2). \end{aligned}$$

Therefore:

$$\mu_a - \mu_g = \mu_a \left(1 - \exp \left(-\frac{\sigma^2}{2\mu^2} \right) \right) + o(\sigma^2). \quad (9)$$

When $\frac{\sigma^2}{2\mu^2}$ is small, this can be approximated as:

$$\Delta \approx \frac{\sigma^2}{2\mu_a} \quad (10)$$

□

Theorem A1 (Scaling Law for Downstream Task Performance). *Consider a language model M_C trained with compute budget C and a set of downstream tasks \mathcal{P} . Under the following assumptions: Assumption 1 (Power-law scaling of answer loss): the expected answer loss follows:*

$$L_{\mathcal{P}}(C) := \mathbb{E}_{(q, a_{true}) \sim \mathcal{P}} [L(q, a_{true}; C)] = \alpha C^{-\beta} + \gamma \quad (11)$$

where $\alpha, \beta, \gamma > 0$ are task-specific constants, with γ representing the irreducible loss.

Assumption 2 (Unique deterministic answers): Each question has a unique deterministic answer. The model receives score 1 if and only if M_C outputs a_{true} , and 0 otherwise.

Assumption 3 (Accuracy decomposition): The expected accuracy decomposes as:

$$\mathbb{E}_{T \sim \mathcal{P}}[\text{Acc}(C)] = g + (1 - g) \cdot \mathbb{E}_{(q, a_{\text{true}}) \sim \mathcal{P}}[p(a_{\text{true}}|q, M_C)], \quad (12)$$

where $g \in [0, 1]$ is the random guessing baseline.

Then, the expected accuracy on task set \mathcal{P} can be modeled as:

$$\mathbb{E}_{\mathcal{P}}[\text{Acc}(C)] = g + (1 - g) \left(\exp(-\alpha C^{-\beta} - \gamma) + \frac{\sigma_L^2(C)}{2\mu_L(C)} \right) + o(\sigma_L^2(C)) \quad (13)$$

where $\mu_L(C) = \mathbb{E}_{(q, a_{\text{true}}) \sim \mathcal{P}}[L(q, a_{\text{true}}; C)]$ is the mean loss and $\sigma_L^2(C) = \text{Var}_{(q, a_{\text{true}}) \sim \mathcal{P}}[L(q, a_{\text{true}}; C)]$ is the loss variance across the task set.

Proof. For a task $T = (q, a_{\text{true}}) \in \mathcal{P}$, under assumption 2, a_{true} is deterministic and unique, thus $p(a_{\text{true}}|q, M_C)$ can be decomposed into token-wise auto-regressive loss.

$$-\log(p(a_{\text{true}}|q, M_C)) = -\log \left(\prod_{i=1}^k p(t_i|q, t_{<i}; M_C) \right) \quad (14)$$

$$= -\sum_{i=1}^k \log(p(t_i|q, t_{<i}; M_C)) \quad (15)$$

$$= L(q, a_{\text{true}}; C). \quad (16)$$

Then take the exponential of both sides, and then take the expectation with respect to different tasks in the evaluation set $p = (q, \text{ans}) \in \mathcal{P}$. We note that both p_{ans} and loss_{ans} are functions of C .

$$\mathbb{E}_p[p(a_{\text{true}}|q, M_C)] = \mathbb{E}_p[\exp(-L(q, a_{\text{true}}; C))] = \frac{1}{n} \sum_{(q, a_{\text{true}}) \in \mathcal{P}} \exp(-L(q, a_{\text{true}}; C)). \quad (17)$$

We can adopt [lemma 1](#) to switch from arithmetic mean to geometric mean of loss, and apply the power law assumption 1.

$$\frac{1}{n} \sum_{(q, a_{\text{true}}) \in \mathcal{P}} \exp(-L(q, a_{\text{true}}; C)) = \exp \underbrace{\left(-\frac{1}{n} \sum_{(q, a_{\text{true}}) \in \mathcal{P}} L(q, a_{\text{true}}; C) \right)}_{\text{use loss scaling law}} + \frac{\sigma_L^2(C)}{2\mu_L(C)} + o(\sigma_L^2(C)) \quad (18)$$

$$= \exp(-\alpha C^{-\beta} - \gamma) + \frac{\sigma_L^2(C)}{2\mu_L(C)} + o(\sigma_L^2(C)) \quad (19)$$

where n in the number of tasks in \mathcal{P} , and μ, σ^2 follow definitions in the proposition.

Finally, we use assumption 3 to align the answer passrate and the accuracy metric.

$$\mathbb{E}_{T \sim \mathcal{P}}[\text{Acc}(C)] = g + (1 - g) \cdot \mathbb{E}_{(q, a_{\text{true}}) \sim \mathcal{P}}[p(a_{\text{true}}|q, M_C)] \quad (20)$$

$$= g + \frac{(1 - g)}{n} \sum_{(q, a_{\text{true}}) \in \mathcal{P}} \exp(-L(q, a_{\text{true}}; C)) \quad (21)$$

$$= g + (1 - g) \left(\exp(-\alpha C^{-\beta} - \gamma) + \frac{\sigma_L^2(C)}{2\mu_L(C)} \right) + o(\sigma_L^2(C)) \quad (22)$$

□

Table A1 Prediction errors (EE \downarrow , FE \downarrow) across criteria of extrapolatable subsets.

Metric / Task Set	Baseline		Ablate a	Ablate b	Ablate c	w/o threshold				
	EE \downarrow	FE \downarrow	($a > 0.5$)	($b > 0.05$)	($0 \leq c < 0.5$)	EE \downarrow	FE \downarrow			
Mean	1.18	1.63	1.18	1.67	1.19	1.63	1.44	1.97	2.39	2.36
Max	2.20	2.23	2.20	2.23	2.20	2.23	2.88	2.99	6.24	5.97
GSM8k	2.20	2.23	2.20	2.23	2.20	2.23	1.82	2.01	2.20	2.23
MATH	1.14	1.28	1.14	1.28	1.14	1.28	1.14	1.28	0.80	0.79
BBH	0.29	1.77	0.29	1.77	0.29	1.77	0.21	2.99	6.24	5.97
TriviaQA	1.58	1.64	1.59	1.93	1.58	1.64	1.07	1.17	2.92	3.52
MBPP	1.56	2.19	1.56	2.19	1.56	2.19	1.56	2.19	1.53	1.11
AGIEval	1.11	2.38	1.11	2.38	1.11	2.38	0.08	1.59	2.22	2.65
DROP	0.26	0.23	0.26	0.23	0.32	0.18	2.72	1.68	2.20	1.57
MMLU-pro	1.27	1.35	1.27	1.35	1.27	1.35	2.88	2.86	1.00	1.03

Rationality of Assumption 3 Assumption 3 is designed to accommodate tasks with finite answer sets. For such tasks, when calculating $\text{Acc}(C)$, possibilities outside the answer set are disregarded. When $p(a_{\text{true}} | q, M_C)$ approaches 0, $\text{Acc}(C)$ is at the level of a random guess, g . When $p(a_{\text{true}} | q, M_C)$ approaches 1, $\text{Acc}(C)$ is close to $p(a_{\text{true}} | q, M_C)$. This assumption implies a linear relationship between $\text{Acc}(C)$ and the probability in the $(0, 1)$ interval. The theorem itself is also effective for tasks with open answer sets, where the probability of a correct random guess can be assumed to be 0 (i.e., $g = 0$).

C Additional Ablation Studies

C.1 The Criteria for Extrapolatable Subsets

The criteria for fitting the extrapolation formula (Eq. (4)) are designed to ensure the following:

- 1 $a > 0$ and $b > 0$: These ensure that accuracy is an increasing function of compute. Larger values of a and b signify that task performance scales more distinctly with compute, leading to fitting curves with better scaling properties and differentiability.
- 2 $c \geq 0$: This ensures the extrapolated curve’s maximum value is less than or equal to 1. An excessively large c implies that the fitting curve has a very low ceiling, which is characteristic of task subsets with poor scaling properties. These are thus considered non-extrapolatable.

We conducted an ablation study on these parameters, as shown in Tab. A1. Starting from our baseline criteria ($a > 1$, $b > 0.1$, $0 \leq c < 1$), we individually relaxed the constraints on a , b , and c , and also observed the effect of removing the thresholds entirely.

When the thresholds are removed entirely, the prediction performance degrades significantly. This is because numerous task clusters with poor scaling properties are included in the extrapolation, impairing the overall result. In contrast, individually relaxing the thresholds for a , b , or c still largely preserves the integrity of the filtering criteria. The performance shows only a slight drop compared to the baseline, indicating that while the filtering step is important, our method is not overly sensitive to the specific threshold values.

C.2 Interpolation Method

To evaluate different interpolation methods for prediction accuracy, we compared various mathematical approaches. Our baseline method uses quartic polynomial interpolation, which we compare against several alternative approaches, including Cubic spline interpolation, Cubic polynomial interpolation, and Quintic polynomial interpolation.

The comparative results across different benchmarks are shown in Tab. A2. We report the prediction error between the real performance of a large model and the mapping result.

Table A2 Comparison of different interpolation methods across benchmarks.

Prediction Error	BBH	Math	MMLU-pro
Cubic Spline	0.68	1.31	1.37
Cubic Polynomial	3.38	1.12	1.35
Quintic Polynomial	0.18	1.42	1.36
Quartic Polynomial	1.77	1.28	1.35

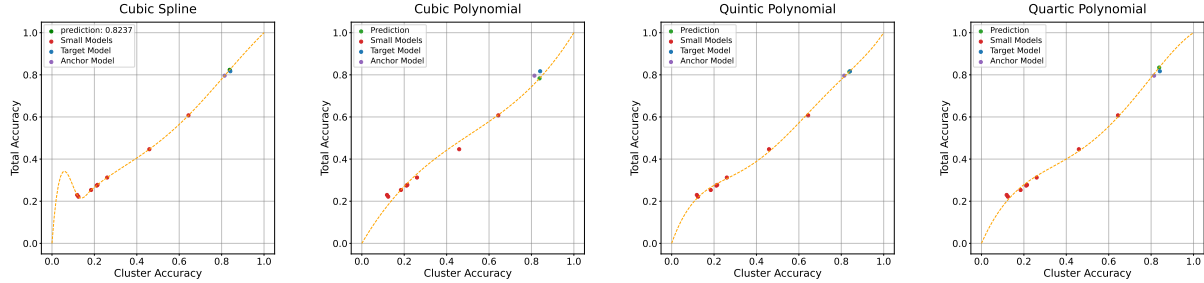


Figure A1 Performance mapping with different interpolation methods on the BBH evaluation set. The cubic spline is overfitted, and the cubic polynomial method is underfitted. Quartic polynomials and quintic polynomials are comparable, while a quartic polynomial has fewer parameters.

Furthermore, in figure A1, we plot the mapping process using different interpolation formulas, where the x-axis represents the predictable subset indices and the y-axis represents the full set indices. The red points are the numerical values to be fitted, green points represent predicted values, purple points represent anchor points, and blue points show the actual performance.

The prediction performance shows certain robustness across different interpolation methods. We aim to use the simplest possible interpolation function while maintaining low prediction errors. Based on the above results, we observe that the Cubic Polynomial shows larger prediction errors due to underfitting on BBH, while the Cubic Spline exhibits some overfitting. Both Quartic Polynomial and Quintic Polynomial perform well, therefore, we chose the Quartic Polynomial method as it requires fewer fitting parameters.

When the number of small models used for fitting varies, the polynomial form also needs to be adaptively adjusted to ensure the robustness of the mapping. For instance, in the experiment of predicting the 12B model, the scaling function was adjusted from a quartic polynomial to a cubic polynomial to mitigate overfitting.

C.3 Different Anchor Points in Interpolation Mapping

We find that the mapping relationship from predictable subset metrics to full evaluation set metrics is similar across models with different training data and architectures. This allows leveraging pre-trained models as "anchors" to refine the mapping and improve final estimation accuracy. We use Qwen2-72B [45] (OOD anchor) and an in-house MoE model [26] with the same training data but different architecture (ID anchor). We first derive an interpolation curve using only small model metrics and fixed points $(0, 0)$, $(1, 1)$, then assess anchor compatibility. This shared mapping implies estimable subset metrics are highly correlated with full-set metrics and less prone to interference from other model parameters than loss-intermediate predictions.

We test three configurations:

- COD (w/o anchor): Full COD pipeline, but no anchor points in the mapping phase;
- COD (w. OOD anchor): COD with Qwen2-72B as an out-of-distribution anchor;
- COD (w. ID anchor): COD with our in-house MoE model as an in-domain anchor.

Tab. A3 shows that incorporating either OOD or ID anchors consistently enhances prediction accuracy. This suggests a stable correlation between predictable subset and full-set metrics across diverse models, enabling

Table A3 Influence of anchor points in the mapping stage on prediction error (pp). Lower is better.

Method	Overall		Individual Task Sets							
	Mean↓	Max↓	GSM8k	MATH	BBH	TriviaQA	MBPP	AGIEval	DROP	MMLU-pro
w/o. anchor	3.96	8.80	2.17	5.46	5.08	1.68	8.80	2.38	4.44	1.68
w. OOD anchor	1.59	2.56	2.22	0.94	1.84	1.04	2.56	1.86	1.18	1.04
w. ID anchor	1.63	2.38	2.23	1.28	1.77	1.64	2.19	2.38	0.23	1.35

Table A4 Model architecture specifications across different sizes.

	122M	238M	411M	652M	973M	1.9B	7B	12B	70B (Target)
Param. (M)	122	238	411	652	973	1,901	6,980	12,022	68,452
Compute Per Token (B)	1.535	2.684	4.275	6.378	9.060	16.436	54.761	91.609	475.131
Tokens (B)	26	45	72	108	153	277	923	1,544	8,012
Continue-Trained Tokens (B)	3	5	8	12	18	33	114	191	1,000
Model Dimension	1,024	1,280	1,536	1,792	2,048	2,560	4,096	4,608	8,192
FFN Dimension	3,584	4,480	5,376	6,272	7,168	8,960	14,336	16,128	28,672
Heads	8	10	12	14	16	20	32	36	64
KV Heads	8	10	12	14	16	20	8	12	8

the use of existing model evaluations to improve predictions for new models. Furthermore, since our clustering identifies intrinsic properties of evaluation sets, the derived predictable subsets are applicable to new models. Additional ablations on the interpolation method (Sec. C.2) confirms quartic functions are suitable.

D Experimental Settings and Training Recipe

Training recipe. To establish performance predictions for large language models, we conduct systematic experiments with a suite of smaller-scale models across different parameter counts. All our models are trained from scratch on a corpus of text data. We do not fix the data budget for all models; instead, we maintain a consistent Data-to-CPT (Compute per token) ratio for all models, as mentioned in Sec. 5.1. We list model configurations in Tab. A4.

We adopt the in-house training data that comprises multilingual text corpora, with increased weighting for domains such as STEM, code, and general knowledge, following Llama3 [17], Deepseek-v2 [28], Fineweb-EDU [29], etc. We apply several de-duplication methods and data cleaning mechanisms to each data source to ensure high-quality tokens.

The model architecture is consistent with Llama3.1 [17], incorporating Grouped-Query Attention (GQA) [2], SwiGLU activation function [35], RMSNorm [48] with Pre-normalization, etc. The models are trained using BF16 precision with a sequence length of 8192 and a RoPE [37] base of 500,000. We employ the AdamW optimizer with $\beta = (0.9, 0.95)$, a weight decay of 0.1, and a dropout rate of 0.1.

All models are trained on a constant learning rate scheduler with a few-step warmup stage. To determine the learning rate and batch size, we adopt the hyperparameter scaling laws from Liu et al. [28]. Specifically, the optimal learning rate η_{opt} , and the optimal batch size B_{opt} are defined as power laws of the compute, measured in FLOPs: $\eta_{opt} = a_1 \cdot C^{-b_1}$ and $B_{opt} = a_2 \cdot C^{b_2}$, where a_1, b_1, a_2, b_2 are parameters to be fitted. We perform a grid search on our small models to identify their optimal learning rates and batch sizes, and then extrapolate these findings to the bigger models.

Training Resources. The 7B dense model is trained on 923B tokens, consuming 52,800 H800 GPU-hours. The computational resources used for the other models can be estimated proportionally based on their respective compute requirements.

Evaluation settings and protocol. We conducted performance scaling estimation experiments across eight major LLM evaluation sets. These evaluation sets span a diverse range of capabilities, including Math, Reasoning,

Table A5 Information of evaluation datasets.

Dataset	Domain	#Questions	#Shots
GSM8K	Math	1,319	8
MATH	Math	5,000	4
BBH	Reasoning	6,511	3
TriviaQA	Knowledge	17,944	5
MBPP	Coding	500	3
AGIEval	Comprehensive	8,063	5
DROP	Reading	9,536	3
MMLU-pro	Comprehensive	12,032	5

Knowledge, Coding, Reading, and general abilities. All pretrained LLMs were evaluated using a few-shot methodology to obtain the performance metrics. Detailed information is provided in Tab. A5. Our evaluation methodology aligns with that used for the Llama3 [17] pre-trained models. We assess the models’ capabilities directly through few-shot text completion tasks without any instruction tuning or Supervised Fine-Tuning (SFT). This evaluation method is chosen because even a small amount of SFT data can significantly influence performance on downstream tasks, thereby not reflecting the inherent capabilities of the pre-trained model itself.

Software Framework. All models are trained using the Megatron framework. The evaluation code is an in-house implementation designed to be consistent with the Llama3 [17] evaluation methodology.

E Additional Prediction Results for a Medium-size Model

The COD method is also effective for predicting the capabilities of medium-size language models. To demonstrate this, we conducted an experiment to predict the performance of a 12B model using source models ranging from 122M to 1.9B parameters. This setup maintains a similar $6 \times$ parameter-size ratio as our main experiment (predicting 70B from models up to 12B).

For this experiment, clustering relied exclusively on the passrate@100 data from the 122M to 1.9B source models to prevent data leakage from the target model. The results in Tab. A6 show that COD is more robust and less demanding on the size of source models compared to the baselines. For instance, the baseline methods perform poorly on the BBH benchmark, In contrast, COD accurately captures the trend of accuracy growth as compute increases and yields precise extrapolations. We will include a plot of this curve in the main text to visually demonstrate the clear advantage of COD.

The prediction errors of all methods for the 12B model are significantly higher than those for the 70B model reported in Sec. 5.2. Extrapolation accuracy improves when larger source models are employed for fitting, as a greater number of samples have “emerged”. If the largest source model is excessively small, numerous samples remain “unemerged”, resulting in substantial errors when extrapolating to a significantly larger model.

F Performance Prediction for Continue-Pretrained LLMs

Leading industry pre-trained LLMs (e.g., Deepseek-v3 [10], Llama3 [17], Qwen-2.5 [44]) adopt the Continual Pre-Training (CPT) strategy of concentrating high-quality data towards the end of the pre-training process. This phase is typically accompanied by learning rate decay, enabling the model to fully absorb this high-quality data. Due to significant changes in data distribution and the learning rate schedule, this approach often yields substantial improvements in metrics. Predicting a large model’s final capability based solely on its performance during a “stable” phase with consistent data distribution does not reflect its ultimate capability. Therefore, we supplement this by providing metric predictions for the high-quality CPT phase.

The relationship between model parameter scale and the volume of CPT tokens is listed in Tab. A4.

We conduct the same COD pipeline for CPT models. We control the data distribution of the stable and decay

Table A6 Absolute prediction error (%) on evaluation sets for predicting the performance of the 12B model. Errors $< 2\%$ are considered accurate (green), while errors $> 5\%$ are considered invalid (red). \downarrow indicates lower is better.

Task Sets/Metrics	Ground Truth	Loss-intermediate		End-to-end		BNSL		COD	
		Prediction	Error	Prediction	Error	Prediction	Error	Prediction	Error
Overall Metrics									
Mean	-	-	14.92	-	10.52	-	17.42	-	4.68
Max	-	-	23.82	-	24.43	-	28.26	-	10.39
Individual Task Sets									
GSM8k	70.47	60.86	9.61	63.66	6.81	80.99	10.52	60.08	10.39
MATH	30.85	41.53	10.68	34.36	3.51	49.26	18.41	28.48	2.37
BBH	60.76	36.94	23.82	36.33	24.43	36.10	24.66	57.751	3.05
TriviaQA	58.84	68.42	9.57	59.88	1.04	87.10	28.26	57.92	0.93
MBPP	47.80	28.53	19.27	36.51	11.29	27.95	19.85	44.50	3.30
AGIEval	44.13	33.91	10.22	35.40	8.74	34.12	10.01	47.53	3.40
DROP	54.35	35.05	19.30	37.19	17.16	36.73	17.62	63.50	9.14
MMLU-pro	37.60	20.74	16.86	26.41	11.20	27.59	10.01	42.42	4.82

phases for various smaller models, as well as their token-to-parameter ratio, to be consistent with the large model targeted for prediction. The last checkpoint is used for evaluation. Based on prior clustering labels, we perform fitting, extrapolation, and mapping to obtain the predicted performance for the large model.

Table A7 Predicted vs. actual metrics for an LLM with 70B parameters after high-quality continued pretraining.

Evaluation Set	Predicted Metric	Actual Metric	Prediction Error
MMLU-pro	61.58	59.34	2.24
BBH	84.66	85.32	0.66
TriviaQA	79.64	84.05	4.41
MBPP	73.00	73.20	0.20
AGIEval	61.66	64.18	2.52
DROP	81.65	81.39	0.26
GSM8k	86.88	91.81	4.93
MATH	49.29	52.68	3.39

Results listed in Tab. A7 show that the proposed COD method achieves an average prediction error of 2.33%.

We observe that MATH, GSM8k, and TriviaQA exhibit relatively large prediction errors. We hypothesize that there are two main categories of reasons for this inaccuracy:

1. The CPT data and the evaluation sets possess a significant correlation. For example, in math-related evaluation sets, a modest amount of training can yield substantial improvements in performance metrics. In such scenarios, the metrics for smaller models tend to show greater volatility and have inaccurate evaluations.
2. The CPT data exhibits inherent distribution bias, such that certain evaluation sets, such as TriviaQA, do not derive performance gains from it. This leads to potential significant fluctuations in the metrics after the CPT phase, thereby diminishing the accuracy of extrapolating to larger models.

G Difficulty Distribution of Predictable Subset

We analyze the proportion of predictable subset tasks across different difficulty levels. The difficulty distributions of predictable subset versus complete sets for different evaluation benchmarks are illustrated in figure A2. We use the scores from the 12B model as the basis for difficulty classification. The results show

that MMLU-pro and GSM8k evaluation sets have larger proportions of predictable subsets, indicating that most questions in these datasets exhibit good performance scaling properties. In contrast, many difficult questions with near-zero scores in the MATH evaluation set fall outside the predictable subset, requiring adjustment during the mapping phase. Meanwhile, BBH exhibits consistent proportions of its predictable subset across varying difficulty levels, as some questions display oscillatory patterns with limited improvement, even with increased computational resources.

The proportion of the predictable subset can serve as a metric for assessing evaluation set quality. Evaluation sets with larger predictable subsets yield more reliable experimental conclusions from smaller models. When constructing evaluation sets, we recommend screening or supplementing unpredictable clusters and ensuring a minimum number of questions for each difficulty feature to reduce metric volatility.

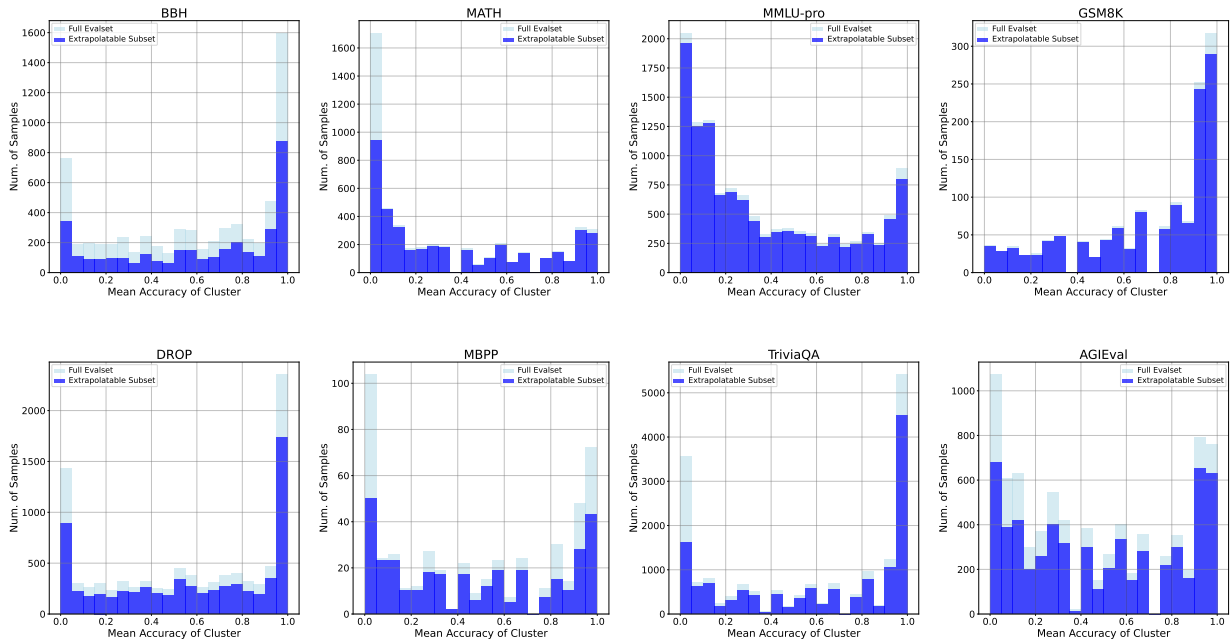


Figure A2 Difficulty distribution comparison on a 12B model between predictable subset and full evaluation set.

H Computational Cost

The extra computational overhead of running COD is not expensive compared to training a series of small models with increasing parameter sizes. The main additional cost comes from performing 100 inference evaluations on the evaluation set for each small model (the cost of clustering algorithm is negligible compared to the inference cost). The computational complexity is $O(TMN)$, where T is the number of evaluation runs, M is the number of tokens for one evaluation, and N is the maximum parameter size of the small models used for prediction. The corresponding token usage is $O(TM)$.

In particular, for an evaluation set requiring $1M$ tokens, a total of $100M$ tokens for small model inference is needed. In our experiments, the training token count for the 12B small model is $1.554T$. Considering that a training token is typically 3 times more costly than an inference token, the additional cost of COD is approximately $\frac{100M}{1.554T \cdot 3} \approx 0.002\%$ of the training cost.

I Limitations

Influence of model structure. Mixture-of-Experts (MoE) models excel in training and inference cost, and are widely used in production. In this work, we reveal the performance scaling on dense transformers, while

prediction on MoE models is still underexplored. However, we believe that the proposed method is not significantly affected by the model architecture. We expect similar results for MoE models.

Category of evaluation sets. The proposed Clustering-on-Difficulty method requires a sufficient number of test cases, as too few samples can lead to unstable cluster metrics and ineffective estimation. From an evaluation set design perspective, an evaluation set with good predictive properties enables more effective generalization from small-scale to large-scale models, thus providing better guidance for model iteration.

Furthermore, for multiple-choice tasks, the model only needs to assign a higher probability to the correct option compared to others, creating a discrepancy between the answer loss and the model’s true passrate. Given that more evaluation sets are adopting Chain-of-Thoughts prompts, we have not included multiple-choice tasks that only require option selection.

Chain-of-thought performance prediction. [theorem 1](#) assumes that evaluation sets directly assess models’ ability to provide answers. However, increasingly more evaluations allow models to think before providing answers. Recent works on inference time scaling [5, 36] further demonstrate that for tasks involving mathematics, reasoning, and coding, training models to complete tasks through longer inference computation can significantly improve downstream task performance. In cases where the reasoning process or answers are not unique, the relationship between a model’s answer loss and passrate on a task may not necessarily follow the exponential relationship between the answer loss and the sample passrate. Although our approach maintains its prediction effectiveness in such situations, the theoretical explanation for these cases is insufficient. Therefore, we consider improving prediction methods based on chain-of-thought characteristics and expanding theoretical foundations as future work.